Chemical Engineering Journal 143 (2008) 195–200

Contents lists available at ScienceDirect

Chemical Engineering Journal

journal homepage: www.elsevier.com/locate/cej

Heat and mass transport in a nonlinear fixed-bed catalytic reactor: Hot spots and thermal runaway

Redhouane Henda[a,*], Alan Machac[a], Bernt Nilsson[b]

[a] School of Engineering, Laurentian University, Sudbury, ON P3E 2C6, Canada
[b] Department of Chemical Engineering, Lund University, 221 00 Lund, Sweden

ARTICLE INFO

Article history:
Received 20 September 2007
Received in revised form 23 March 2008
Accepted 10 April 2008

Keywords:
Transient behavior
Heat and mass transport
Exothermic reaction

ABSTRACT

Transient heat and mass transport in a wall-cooled tubular catalytic bed reactor is numerically investigated. A two-dimensional pseudo-heterogeneous model, accounting for transport in the solid and fluid phases, with axial and radial dispersions is used to describe transport in the reactor. The effects of inlet process conditions, viz., temperature and concentration, are investigated and their impact on the development of thermal runaway and hot spots in the reactor is analyzed. Under typical process conditions the calculation results show the development of a hot spot downstream the reactor inlet. At reduced feed temperature thermal runaway develops for an inlet concentration of 0.505 mol/m^3. A criterion for thermal runaway limit has been developed whereby runaway can be detected at a point in time during the process when the time derivative of temperature increases monotonously with time throughout the bed. Under low feed concentration and temperature a simpler pseudo-homogeneous model can be used to describe the reactor.

1. Introduction

Fixed-bed catalytic reactors serve as the workhorse of the chemical industry with widespread use in economic sectors of vital importance such as petroleum refining, chemicals manufacturing, and environmental clean-up. Exothermic reactors, such as those used for oxidation and hydrogenation reactions, are generally operated under process conditions that potentially give rise to a rich palette of nonlinear behaviors, e.g., multiple steady-states, hot spot, and runaway. These are fundamentally due to strong feedback mechanisms between various transport phenomena – namely, heat and mass transfers – and chemical reaction kinetics, and depend on operation conditions, e.g., see [1–4] and references therein. While fixed-bed reactors, relatively to other types of catalytic reactors, are flexible, efficient, low-cost, and require low maintenance, their most serious disadvantage is poor heat transfer with attendant poor temperature control [4]. Heat transfer and temperature control can be facilitated through external or internal heat exchange and a judicious choice of process parameters. Owing to the large number of design parameters in such processes there has been a concerted research effort to gain a better understanding of their behaviors and performance. While the rate of chemical reactions is generally a complex exponential function of temperature, if no or inadequate cooling is applied to the reactor, the temperature will increase very rapidly along the reactor potentially resulting in a temperature spike or hot spot [5]. This phenomenon can cause damage to both catalyst (via sintering) and reactor vessel (via thermal stresses). Consequently, the operation of such processes may incur high maintenance costs, staggering safety, and loss in productivity. Process selectivity may also deteriorate through the initiation of undesired side chemical reactions. In addition to the development of a hot spot in the reactor, the latter can also be prone to large parametric sensitivities, or thermal runaway, due to the inherent feedback mechanism. However, running the reactor near thermal runaway conditions is potentially advantageous to the catalytic process as it may result in optimum reactor operation. This is especially attractive if energy savings can be attained.

Experimental observations of nonlinear behaviors in catalytic reactors are still scarce. Hot spots have been reported in commercial packed-bed reactors [6,7], and recently rotating thermal patterns have been observed on a cylindrical surface with radial flow catalyzing carbon monoxide oxidation on a platinum/alumina catalyst [8]. Difficulties encountered in experimental observation of nonlinear behaviors have triggered an increasing need for a fundamental understanding of catalytic reactors using mathematical modeling. There are two main categories of reactor models in use: the homogenous model in which gradients between the phases are neglected, and the heterogeneous model, which accounts for both phases and transport exchange between them. Both models are based on the volume averaging of constitutive transport equations

* Corresponding author. Tel.: +1 705 675 1151; fax: +1 705 675 4862.
E-mail address: rhenda@laurentian.ca (R. Henda).

1385-8947/$ – see front matter.
doi:10.1016/j.cej.2008.04.015

Nomenclature

a	specific area (m^2/m^3)
Bi	Biot number (−)
cp	heat capacity (J/K/mol)
C	dimensionless molar concentration (−)
D	diffusivity (m^2/s)
Da	Damköhler number (−)
E_a	activation energy (J/mol)
ΔH_r	heat of reaction (J/mol)
ΔH_i^{ads}	heat of adsorption of i (J/mol)
k	thermal conductivity (W/m/K)
L	reactor length (m)
p, p_i	pressure, partial pressure (Pa)
Pe	Peclet number (−)
r	radial coordinate (−)
R	dimensionless reaction rate (−)
$\Re$	reaction rate (mol/kg/s)
Re	Reynolds number (−)
R_g	gas constant (J/K/mol)
R_t	tube radius (m)
St	Stanton number (−)
t	dimensionless time (−)
T	temperature (K)
u_o	fluid superficial velocity (m/s)
z	axial coordinate (−)

Greek letters

ε	void fraction (−)
ν	CO stoichiometric coefficient (−)
θ	dimensionless temperature (−)
$\Delta\theta^*_{ad}$	adiabatic temperature rise (K)
ρ	density (kg/m^3)

Subscripts

a	axial
eff	effective
f	fluid
h	heat
i	species i
in	inlet
m	mass
p	particle
r	radial
s	solid
t	tube

Superscripts

ads	adsorption
*	absolute quantity
◦	pre-exponential constant

[9]. Generally, homogeneous models, due to their relative simple numerical implementation, have been used most for the description of fixed-bed reactors but not without serious shortcomings, especially when inter-phase thermal and concentration gradients exist. In a previous study of a fixed-bed reactor, with the same model reaction as the one used in the present work and at reactor inlet temperature of 385 K, a pseudo-homogeneous model without axial dispersion was found to be inadequate to describe the thermal behavior of the reactor [10]. In the present work we extend the previous study by using a transient pseudo-heterogeneous model to describe transport in the reactor under various reactor inlet conditions. The pseudo-heterogeneous model, which recognizes the two-phase nature of the system, is more suitable than the pseudo-homogeneous model. The effective transport parameters in this model still lump the heat transport in both phases, whilst the reaction rate is calculated using the temperature of the solid phase [11].

This study aims at investigating transient heat and mass transport in a two-dimensional tubular fixed-bed catalytic reactor using numerical modeling. The effects of process conditions, namely temperature and concentration, at the reactor inlet are investigated and their impact on the dynamic behavior of the system in question is analyzed. The focus is on hot spot and thermal runaway development in the reactor. The suitability of a pseudo-homogeneous model for the description of transport in the reactor is also discussed.

2. Reactor model and data

2.1. Model formulation

The system consists of a packed bed of catalyst (s: solid phase, hereafter) and gaseous reactants (f: fluid phase, hereafter). The reactor tube is placed in a cooling jacket. A simple cross-sectional view of the reactor system is illustrated in Fig. 1. In the present work, we consider the well-documented exothermic oxidation reaction of carbon monoxide, CO, into carbon dioxide, CO_2, over copper chromite as the catalyst [10,12,13]. See the Appendix A for further details. The pseudo-heterogeneous model with axial dispersion describes the reactor via two partial differential equations, account-

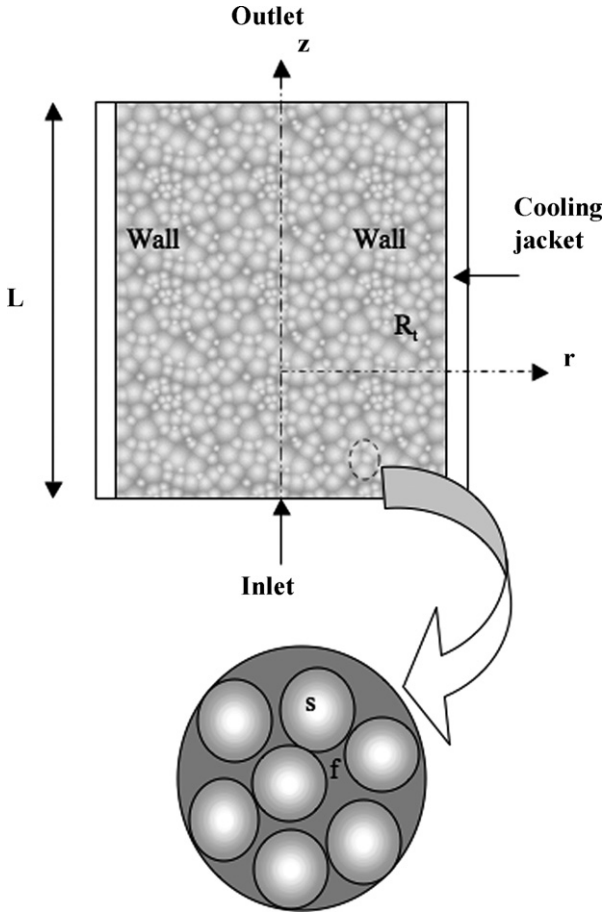

Fig. 1. Simplified schematics of the catalytic fixed-bed reactor.

ing for the mass and energy balances in the fluid phase, and two ordinary differential equations, accounting for the mass and energy balances in the solid phase. A flat radial velocity profile is assumed under the conditions of the present study in accordance with literature data [14]. The transport equations in dimensionless form are given by the following pseudo-heterogeneous model.

Mass balance:

Fluid phase:

$$\varepsilon\, a\frac{\partial C_f}{\partial t} = \frac{1}{Pe_{m,a}}\frac{\partial^2 C_f}{\partial z^2} + \frac{1}{Pe_{m,r}}\frac{1}{r}\frac{\partial}{\partial r}\left(r\frac{\partial C_f}{\partial r}\right) - \frac{\partial C_f}{\partial z} + St_m(C_s - C_f) \quad (1)$$

Solid Phase:

$$(1-\varepsilon)a\frac{dC_s}{dt} = \nu(1-\varepsilon)Da \quad R(C_s,\theta_s) - St_m(C_s - C_f) \quad (2)$$

Energy balance:

Fluid phase:

$$\varepsilon\, a\frac{\partial \theta_f}{\partial t} = \frac{1}{Pe_{h,a}}\left(\frac{\partial^2 \theta_f}{\partial z^2}\right) + \frac{1}{Pe_{h,r}}\frac{1}{r}\frac{\partial}{\partial r}\left(r\frac{\partial \theta_f}{\partial r}\right) - \frac{\partial \theta_f}{\partial z} + St_h(\theta_s - \theta_f) \quad (3)$$

Solid Phase:

$$\frac{(1-\varepsilon)\rho_s c_{p,s}}{\rho_f c_{p,f}} a\frac{d\theta_s}{dt} = (1-\varepsilon)Da \quad R(C_s,\theta_s) - St_h(\theta_s - \theta_f) \quad (4)$$

where C_f and C_s are the dimensionless concentrations of carbon monoxide in the fluid and solid phases, respectively, and θ_f, and θ_s are the dimensionless temperatures of the fluid and solid phases, respectively. The independent variables are the dimensionless time, t, and dimensionless radial, r, and axial, z, coordinates. For the definition of the dimensionless reaction rate, R, see the Appendix A.

Pertinent dimensionless variables and parameters are:

$$r = \frac{r^*}{R_t},\ z = \frac{z^*}{R_t},\ t = \frac{t^*}{t_o},\ C_f = \frac{C_f^*}{C_{in}^*},\ C_s = \frac{C_s^*}{C_{in}^*},\ \theta_f = \frac{\theta_f^* - \theta_{in}^*}{\Delta\theta_{ad}^*},\ \theta_s = \frac{\theta_s^* - \theta_{in}^*}{\Delta\theta_{ad}^*}, \quad (5)$$

$$a = \frac{R_t}{t_o u_o},\ \Delta\theta_{ad}^* = \frac{|\Delta H_r| C_{in}^*}{\rho_f c_{p,f}},\ Bi = \frac{h_w R_t}{k_{r,eff}},\ Pe_{m,a} = \frac{u_o R_t}{D_{a,eff}},\ Pe_{m,r} = \frac{u_o R_t}{D_{r,eff}},$$

$$Pe_{h,a} = \frac{u_o \rho_f c_{p,f} R_t}{k_{a,eff}},\ Pe_{h,r} = \frac{u_o \rho_f c_{p,f} R_t}{k_{r,eff}},\ St_m = \frac{a_p h_m R_t}{u_o},\ St_h = \frac{a_p h_p R_t}{u_o \rho_f c_{p,f}},$$

$$Da = \frac{\rho_s R_t}{u_o C_{in}^*}\Re(C_s,\theta_s)|_{in},$$

where the asterisk denotes variables with absolute values. Parameter $\Delta\theta_{ad}^*$ is the adiabatic rise, i.e., the highest possible temperature rise in the reactor under adiabatic operation and full conversion of the reactant. The dimensionless numbers appearing in the second, third, and fourth rows of Eq. (5) are defined as usual.

Eqs. (1)–(4) are subject to the following initial and boundary conditions:

IC:

$$t = 0,\ C_f = 0,\ C_s = 0,\ \theta_f = 0,\ \theta_s = 0. \quad (6)$$

BCs:

$$z = 0, \forall r, -\frac{\partial C_f}{\partial z} = -Pe_{m,a}(C_f - C_{in}), -\frac{\partial \theta_f}{\partial z} = -Pe_{h,a}(\theta_f - \theta_{in})$$

$$z = \frac{L}{R_t}, \forall r, -\frac{\partial C_f}{\partial z} = 0, -\frac{\partial \theta_f}{\partial z} = 0$$

$$r = 0, \forall z, -\frac{\partial C_f}{\partial r} = 0, -\frac{\partial \theta_f}{\partial r} = 0$$

$$r = 1, \forall z, -\frac{\partial C_f}{\partial r} = 0, -\frac{\partial \theta_f}{\partial r} = Bi(\theta_f - \theta_w)$$

The pseudo-heterogeneous model given by Eqs. (1)–(5), along with the initial and boundary conditions, Eq. (6), is a nonlinear system for which it is not easy to derive an analytical solution. The coupled transport equations have been numerically implemented using Comsol Multiphysics®, a finite-element based software package. The latter has provided for the discretization of the model equations and for their solution through an implicit ODE solver based on the method of lines, whereby only space is discretized. The discretization mesh used in the calculations has been refined by using smaller finite elements and the integration time step has been decreased until the calculated concentration and temperature profiles have become independent of both spatial and time discretization steps.

2.2. Model data

Typical process data and parameters along with kinetic and transport data used in the calculation of the concentration and temperature profiles inside the catalytic bed reactor are listed in Table 1. The packed bed has a tube to particle diameter ratio of 11. Materials properties and effective transport parameters have been estimated using a number of widely known correlations. The literature pertinent to this study is provided by [15–20].

3. Results and discussion

3.1. Inlet temperature = 385 K

The temperature at the reactor inlet, θ_{in}^*, has been set to 385 K while the feed concentration, C_{in}^*, has been changed from 0.5 mol/m^3 to 1.4 mol/m^3. The calculated temperature profile of the fluid phase throughout the catalytic bed reactor at $C_{in}^* = 0.5$ mol/m^3 is shown in Fig. 2. Heat transport is clearly two-dimensional as temperature gradients develop along and across the reactor. A temperature front (hot spot) develops downstream the reactor inlet as well. The value of the hot spot at its maximum is about 85 K near the bed centerline. Fig. 3 illustrates the difference in temperature and concentration between the solid and fluid phases throughout the reactor.

A few points are worth clarifying. The inter-phase temperature difference is quite appreciable and can reach over 20 K before the

Table 1
Geometry, properties, operating conditions, kinetic and transport parameters used in the calculations

L	1 m	ρ_s	10.6 kmol/m^3	b_{CO}^o	6.81×10^{-8} Pa^{-1}	$Pe_{m,r}$	10
R_t	0.02655 m	ρ_f	31.1 mol/m^3	ΔH_{CO}^{ads}	30.60 kJ/mol	$Pe_{h,a}$	2
ε	0.4	cp_f	29.45 J/mol/K	$b_{O_2}^o$	3.08×10^{-5} Pa^{-1}	$Pe_{h,r}$	8
C_{in}^*	0.3–1.6 mol/m^3	cp_s	149.32 J/mol/K	$\Delta H_{O_2}^{ads}$	24.44 kJ/mol	St_h	4.13
u_o	0.1 m/s	k_r^o	39.7 kmol/kg/s	b_{CO}^o	6.81×10^{-8} Pa^{-1}	St_m	1.21
θ_{in}^*	335 K, 385 K	ΔH_r	−23.8 kJ/mol	ΔH_{CO}^{ads}	30.60 kJ/mol	Bi	0.24
θ_w^*	335 K, 385 K	E_a	57.29 kJ/mol	$Pe_{m,a}$	2	Re	683

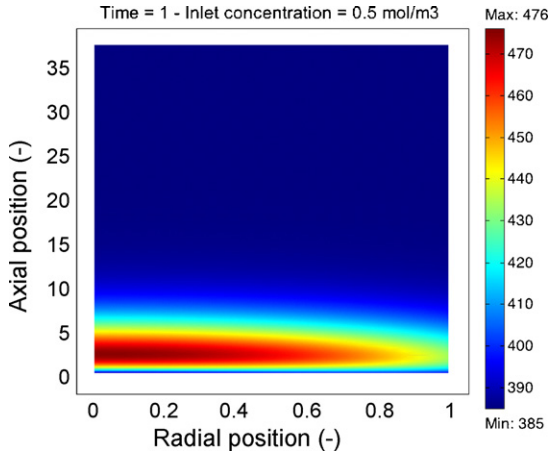

Fig. 2. Fluid temperature profile throughout the reactor for $\theta^*_{in} = 385$ K.

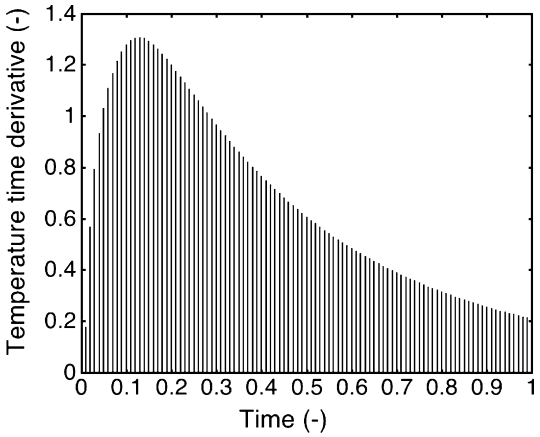

Fig. 4. Evolution of the time derivative of the fluid temperature with time along the centerline at $\theta^*_{in} = 385$ K and $C^*_{in} = 0.5$ mol/m^3.

hot spot region as depicted in Fig. 3a. The magnitude of the concentration difference between the two phases is greatest around the hot spot region as shown in Fig. 3b. The temperature of the hot spot is high enough so that carbon monoxide feed concentration is fully converted immediately downstream the hot spot (see Fig. 3b). These results clearly show that a two-dimensional heterogeneous model is necessary to capture the behavior of the reactor ahead and around the hot spot under the conditions of the present study. The evolution of the fluid temperature with time is depicted in Fig. 4. The latter shows the time derivative of the fluid temperature as a function of time along the reactor centerline. As can be noticed, the envelope of temperature time derivative increases with time initially and then steadily decreases beyond a certain point in time. The concentration–temperature phase plane given in Fig. 5 indicates that the magnitude of the hot spot increases with the inlet concentration of carbon monoxide to reach impractical values, e.g., about 240 K at 1.4 mol/m^3. No sign of thermal runaway could be detected as the inlet concentration range has been swept, viz., from 0.5 mol/m^3 to 1.4 mol/m^3.

3.2. Inlet temperature = 335 K

In this series of calculations the temperature of the feed at the reactor inlet has been decreased and set to 335 K. The feed concentration has been varied between 0.3 mol/m^3 and 1.6 mol/m^3. For a feed concentration of 0.3 mol/m^3 the time derivative of the fluid temperature, as depicted in Fig. 6, shows a dependency on time that is similar to Fig. 4. After an initial increase with time the temperature change relatively to time decreases steadily with time. As the feed concentration is increased thermal runaway appears corresponding to $C^*_{in} = 0.505$ mol/m^3 (see Fig. 7). Thermal runaway has been defined at the inflection point of the temperature profile along the reactor, i.e., $\partial^2\theta/\partial z^2 = 0$, as in a previous study [21]. On Fig. 7 the inflection point is located at the zero of the dashed line ahead of the hot spot. In the resent work, we have noticed that thermal runaway corresponds to a situation where the time derivative of temperature increases monotonously as time goes by. Under the conditions of this study the onset of runaway cor-

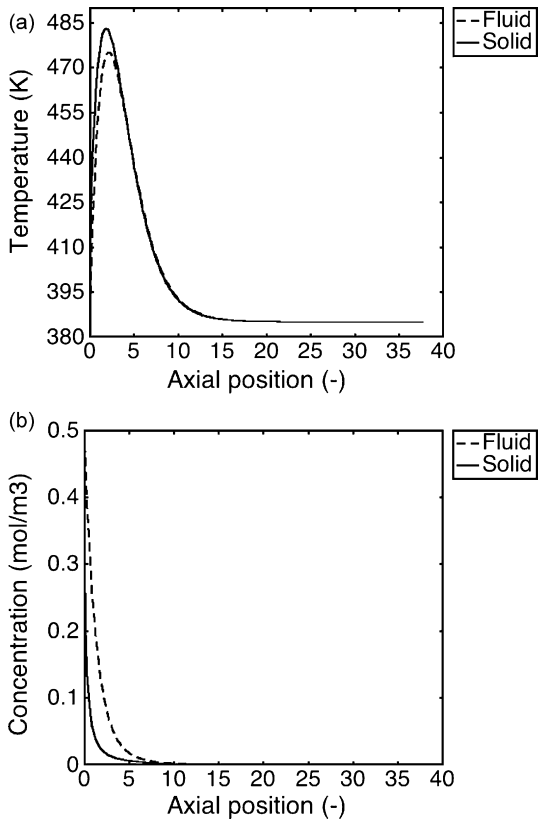

Fig. 3. Temperature (a) and concentration (b) profiles of the solid and fluid phases along the centerline at time = 1, $\theta^*_{in} = 385$ K and $C^*_{in} = 0.5$ mol/m^3.

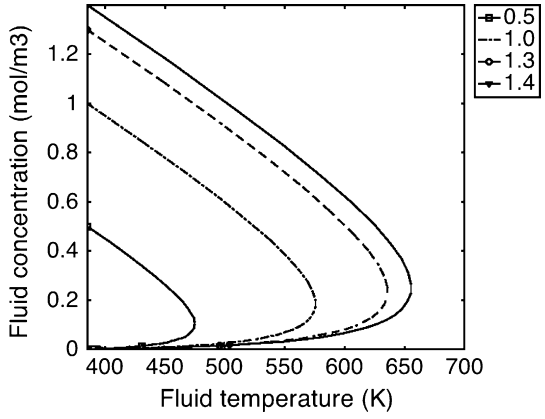

Fig. 5. Concentration–temperature phase plane at various values of the inlet concentration (at the outset) and $\theta^*_{in} = 385$ K.

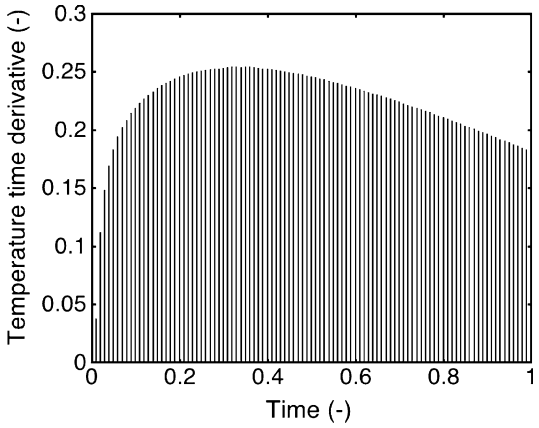

Fig. 6. Evolution of the time derivative of the fluid temperature with time along the centerline at $\theta^*_{in} = 385$ K and $C^*_{in} = 0.3$ mol/m^3.

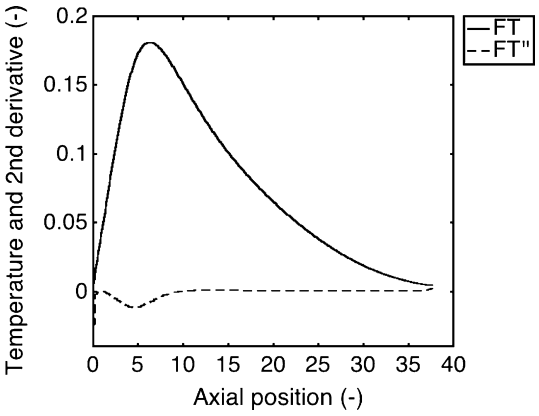

Fig. 7. Fluid temperature (FT) profile and its space second derivative (FT′′) along the reactor at $\theta^*_{in} = 335$ K and $C^*_{in} = 0.505$ mol/m^3.

responds to $C^*_{in} = 0.505$ mol/m^3 for $\theta^*_{in} = 335$ K. Fig. 8 depicts the envelope of the time derivative of the fluid temperature along the reactor centerline. As shown in Fig. 8, at runaway the temperature derivative steadily increases as time goes by. In other words, for thermal runaway to occur $\partial T_f^2/\partial t^2$ must be positive over the entire time interval. The runaway limit is reported in Fig. 9 by a dashed line. As the feed concentration is increased so is the magnitude of the hot spot. This is also accompanied by an incomplete conversion

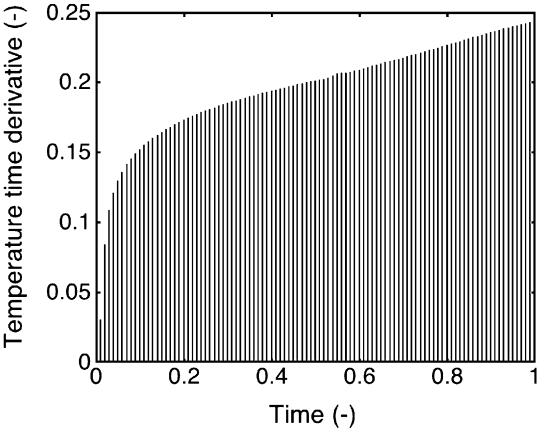

Fig. 8. Evolution of the time derivative of the fluid temperature with time along the centerline at $\theta^*_{in} = 335$ K and $C^*_{in} = 0.505$ mol/m^3.

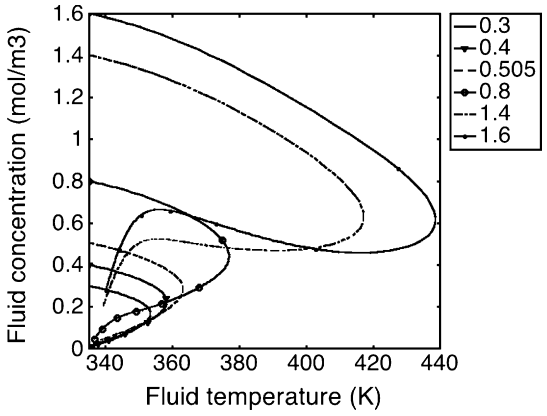

Fig. 9. Concentration–temperature phase plane at various values of the inlet concentration (at the outset) and $\theta^*_{in} = 335$ K.

of carbon monoxide, i.e., conversion value is smaller than unity at reactor exit. From a visual analysis of Fig. 9 the trajectory (not represented) of the maxima in the concentration–temperature curves reaches the maximum at $C^*_{in} = 1.4$ mol/m^3 (dash-dot line).

3.3. Model assessment

Experimental data on packed-bed reactors are quite scarce mainly owing to the difficulty in conducting reliable measurements inherent to this type of reactor. For this work, we have compared calculated CO conversion to measured values available in the literature [22], as shown in Fig. 10. The calculated axial CO conversion profile, using the pseudo-heterogeneous model, is in good agreement with the measured profile. The discrepancies between experimental and calculation data can be substantiated if one considers the fact that heat and mass transfer coefficients reported in the literature are averaged values (semi-empirical) and lump different transport mechanisms of heat and mass. To obtain more accurate transport properties the latter must be derived from experiments under reacting conditions.

We have assessed the validity of the pseudo-homogenous model whose shortcomings have been discussed earlier. The potential of a pseudo-homogeneous model in the description of the thermal behavior of the reactor at high feed temperature ($\theta^*_{in} = 385$ K, in this case) cannot be justified in light of the findings of this work (see Fig. 3). This is true even at low feed concentrations. At the low feed temperature, i.e., $\theta^*_{in} = 335$ K, the pseudo-homogeneous model is again inadequate to describe the behavior of the reactor,

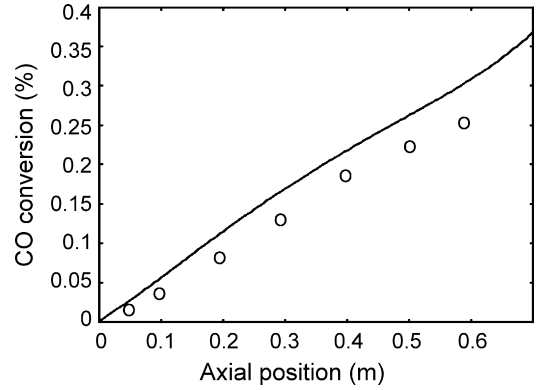

Fig. 10. Comparison between calculated (solid line) and experimental (dots) conversion ($\theta^*_{in} = 375$ K, $C^*_{in} = 1$ vol%, $u_o = 1.2$ m/s).

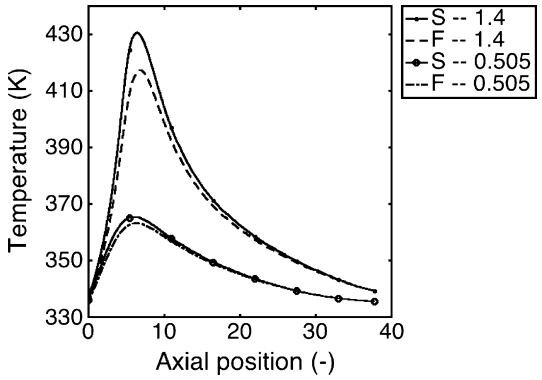

Fig. 11. Temperature profiles of the solid (S) and fluid (F) phases at $C^*_{in} = 0.505\,mol/m^3$ and $1.4\,mol/m^3$ (at the outset) and $\theta^*_{in} = 335\,K$.

especially at high feed concentrations, as shown in Fig. 11. However, up to the runaway limit, corresponding to $C^*_{in} = 0.505\,mol/m^3$, the inter-phase temperature difference does not exceed a few degrees, thus, rationalizing the validity of the pseudo-homogeneous model.

4. Conclusions

We have investigated transient heat and mass transport in a wall-cooled catalytic bed reactor using numerical simulations. A pseudo-heterogeneous model, including axial and radial dispersions, has been used to model transport phenomena. The oxidation reaction of carbon monoxide into carbon dioxide has been selected as model reaction. Under typical process conditions, a hot spot develops downstream the inlet of the reactor. Thermal runaway has been detected for low feed temperature (=335 K) corresponding to a feed concentration of $0.505\,mol/m^3$. The major finding of this work is that thermal runaway can be detected when the space envelope of the time derivative of the temperature increases monotonously with time throughout the reactor. This criterion can be very useful in situations when, for example, the reactor is to be operated near runaway for some time only by manipulating the conditions at the reactor inlet. The results have shown that the pseudo-homogeneous model can only be used at low feed temperature and concentration. In prospective work, the quantitative dynamic criterion of runaway limit will be elucidated.

Acknowledgements

The principal author (R.H.) acknowledges the financial support of the Natural Sciences and Engineering Research Council of Canada and the Center for Chemical Process Design and Control (CPDC) at Lund University (Sweden).

Appendix A

The reaction rate of carbon monoxide conversion over copper chromite ($CO + 1/2O_2 \rightarrow CO_2$, $\Delta H_r = -23.8\,kJ/mol$) is given by the Eley-Rideal mechanism [10], according to which gas phase carbon monoxide reacts with adsorbed oxygen.

$$\Re(C_s, \theta_s) = \frac{k_r b_{CO} p_{CO}}{1 + b_{CO} p_{CO} + b_{O_2} p_{O_2}}$$

where p_i ($i = CO, O_2$) is the partial pressure of i, and

$$k_r = k_r^o e^{-E_a/R_g T},\ b_i = b_i^o e^{\Delta H_i^{ads}/R_g T}$$

The dimensionless reaction rate is defined by

$$R(C_s, \theta_s) = \frac{\Re(C_s, \theta_s)}{\Re(C_s, \theta_s)|_{in}}$$

where the denominator term is the reaction rate at inlet conditions.

References

[1] D. Luss, Temperature fronts and patterns in catalytic systems, Ind. Eng. Chem. Res. 36 (1997) 2931–2944.
[2] M. Sheintuch, S. Shvartsman, Spatiotemporal patterns in catalytic reactors, AIChE J. 42 (1996) 1014–1068.
[3] R. Henda, K. Alhumaizi, Spatiotemporal patterns in a two-dimensional reaction-diffusion-convection system: effect of transport parameters, Math. Comput. Model. 36 (2002) 1361–1373.
[4] C.H. Bartholomew, R.J. Farrauto, Reactors, Reactor Design, and Activity Testing. Fundamentals of Industrial Catalytic Processes, 2nd ed., Wiley, Hoboken, NJ, 2006.
[5] O. Bilous, N.R. Amundson, Chemical reactor stability, AIChE J. (1956) 117–126.
[6] S. Jaffe, Hot spot simulation in commercial hydrogenation processes, Ind. Eng. Chem. Proc. Des. Dev. 15 (1976) 410–416.
[7] C.H. Berkelew, B.S. Gambhir, Stability of trickle-bed reactors, ACS Symp. Ser. 237 (1984) 61.
[8] B. Marwaha, J. Annamalai, D. Luss, Hot zone formation during carbon monoxide oxidation in a radial flow reactor, Chem. Eng. Sci. 56 (2001) 89–96.
[9] S. Whitaker, The Method of Volume Averaging. Theory and Applications of Transport in Porous Media Series 13, Kluwer Academic Publishers, Dordrecht, The Netherlands, 1999.
[10] G.W. Koning, K.R. Westerterp, Modeling of heat transfer in wall-cooled tubular reactors, Chem. Eng. Sci. 54 (1999) 2527–2533.
[11] K.R. Westerterp, W.P.M. van Swaaij, A.A.C.M. Beenackers, Chemical Reactor Design and Operation, Wiley, New York, NY, 1984.
[12] N.J.J. Dekker, J.A.A. Hoorn, S. Stegenga, F. Kapteijn, J.A. Moulijn, Kinetics of the CO oxidation by O_2 and N_2O over Cu-Cr/Al_2O_3, AIChE J. 38 (1992) 385–396.
[13] N.M. Mardanova, R.B. Akhverdiev, R.M. Talyschinskii, A.A. Medzhidov, F.M. Ali-zade, R.G. Rizaev, Oxidation of carbon monoxide on Cu-Cr-Mn/γ-Al_2O_3 catalysts from various sources, Kinet. Catal. 37 (1996) 84–89.
[14] J.G.H. Borkink, K.R. Westerterp, Significance of the radial porosity profile for the description of heat transport in wall-cooled packed beds, Chem. Eng. Sci. 49 (6) (1994) 863–876.
[15] J.B. Agnew, O.E. Potter, Heat transfer properties of packed tubes of small diameter, Trans. Inst. Chem. Eng. 48 (1970) 15.
[16] R. Bauer, E.U. Schlunder, Effective radial thermal conductivity of packings in gas flow. Part I. Convective transport coefficient, Int. Chem. Eng. 18 (1978) 189–204.
[17] B.E. Poling, J.M. Prausnitz, J.P. O'Connell, The Properties of Gases and Liquids, 5th ed., McGraw-Hill, New York, NY, 2000.
[18] M. Elsari, R. Hughes, Axial effective thermal conductivities of packed beds, Appl. Therm. Eng. 22 (2002) 1969–1980.
[19] F.P. Incropera, D.P. DeWitt, Fundamentals of Heat and Mass Transfer, 5th ed., Wiley, New York, NY, 2002.
[20] S. Klemme, J.C. van Miltenburg, Thermodynamic properties of nickel chromite ($NiCr_2O_4$) based on adiabatic calorimetry at low temperatures, Phys. Chem. Miner. 29 (2002) 663–667.
[21] S. Bashir, T. Chovan, B.J. Masri, A. Mukherjee, A. Pant, S. Sen, P. Vijarayaghavan, J. Berty, Thermal runaway limit of tubular reactors, defined at the inflection point of the temperature profile, Ind. Eng. Chem. Res. 31 (1992) 2164–2171.
[22] Koning, B. Heat and Mass Transport in Tubular Packed Bed Reactors at Reacting and Non-reacting Conditions, PhD Thesis (2002), University of Twente.